WETTING KINETICS OF LIQUID ALUMINUM ON AN AL2O3 SURFACE

Zhou, X.B; de Hosson, J.T.M.

Published in:
Journal of Materials Science

DOI:
10.1007/bf00351867

Publication date:
1995

Influence of surface roughness on the wetting angle

X. B. Zhou and J. Th. M. De Hosson
Department of Applied Physics, Materials Science Centre, University of Groningen, Nijenborgh 4, 9747 AG Groningen, The Netherlands

(Received 1 August 1994; accepted 11 April 1995)

In this paper the influence of surface roughness on contact angles in the system of liquid Al wetting solid surfaces of Al_2O_3 has been studied. It was observed that contact angles of liquid Al vary significantly on different rough surfaces of Al_2O_3. A model is proposed to correlate contact angles with conventional roughness measurements and wavelengths by assuming a cosine profile of rough grooves with a Gaussian distribution of amplitudes. In comparison with the experimental results, the model provides a good estimate for describing the influence of surface roughness on contact angles of liquid Al on Al_2O_3.

I. INTRODUCTION

Interface strength between metal and ceramic may be significantly influenced by the wetting behavior on rough surfaces. Rough surfaces may increase the interface area which contributes to an increase of interface strength. On the other hand, a rough surface might not be completely wetted because of poor wetting and sharp grooves. These unwetted parts of the interface may be one of the main reasons for reducing the interface strength.

An accurate measurement of contact angle is important, as the interface energy and the work of adhesion are related to it.[1] However, the contact angle of liquid Al on Al_2O_3 seems to vary significantly for different measurements.[2] The commonly accepted argument for this inconsistency points to the influence of surface oxide layers around liquid Al. Differences in atmosphere or vacuum during wetting experiments contribute to the formation of the oxide layer. However, the deviations of contact angles still varied considerably in some experiments although the vacuum conditions were nearly the same.[2]

Indeed, Al_2O_3 is very hard and difficult to be polished smoothly and since it is usually prepared by sintering, it is porous as well. In that sense the surface of Al_2O_3 is intrinsically rough, an aspect that might affect the experimental values of the contact angle substantially. Despite its importance for (laser) processing and mechanical behavior, effects of surface roughness on the contact angle have not been sufficiently emphasized in the field of metal-ceramic interfaces.

On the other hand, in the study of liquid polymer wetting on a solid, investigations on the effect of surface roughness have been carried out since 1936.[3–5] According to a thermodynamic analysis, Wenzel[3] derived the following formula: $\cos\theta = D\ \cos\theta_{th}$, where D is the roughness parameter which is defined as the average area ratio of real attached interface to its projected part. In his treatment, the rough surface was supposed to be completely wetted by a liquid drop at the interface. However, if the rough surface consists of a sharp groove, the interface will be partly wetted. In addition, Cassie and Baxter[6] derived another equation: $\cos\theta = (1 - F)\cos\ \theta_{th} - F$, where F is the area fraction of an uncontacted solid-liquid interface on solid. However, the equations of Wenzel, Cassie, and Baxter have not been widely accepted in the literature. There are mainly two reasons for this. Firstly, the roughness parameters D and F have not been experimentally realized; i.e., D and F could not be measured experimentally. Secondly, the variation of the experimental contact angles with surface roughness is not consistent with the prediction from the equations of Wenzel, Cassie, and Baxter.[4] Actually, as pointed out by Oliver *et al.*,[4] the equations of Wenzel, Cassie, and Baxter are restricted to a certain special geometry of a rough surface, such as a liquid drop spreading radially on radial grooves, where an equilibrium state can be reached.

However, it is often found that when an interface advances along a surface the advancing contact angle is larger than the receding angle.[7–13] This is known as contact angle hysteresis. Clearly, the interface is not retracing its original path when it recedes, so that the process is not thermodynamically reversible. The existence of hysteresis and irreversibility usually means that a system is trapped in a metastable, nonequilibrium state. Surface roughness is one of the main factors that cause the hysteresis effect. Concentric circular grooves, in the middle of which a liquid drop was placed, contribute to the metastable, nonequilibrium state of wetting, and consequently to the contact angle hysteresis.[7]

In this paper, the effects of these two types of grooves, radial and circular distributions on contact angles, have been examined. A model to correlate contact angles with conventional roughness parameters has been

proposed. Contact angles of liquid Al on various rough surfaces of Al_2O_3 have been measured and the model is applied to analyze the experimental results of liquid Al wetting on rough surfaces of Al_2O_3.

II. EXPERIMENTS

Two sintered Al_2O_3 batches, hereafter called A and B, have been used for wetting experiments. The sintering process and the grain sizes between samples A and B are different, which may contribute to the different behaviors of surface roughness and wetting between them. The as-received Al_2O_3 samples were ground by SiC paper up to 500 grit which are numbered A1 and B1. The smooth samples A2 and B2 were carefully polished by diamond powders of size up to 0.1 μm. The surface of the as-received sample A0 is relatively flat and was used for a wetting test as well. Drop size of pure aluminum is about 1–2 mm in diameter, which is small enough to neglect effects due to gravitation. Wetting experiments were done at 900 °C for 1 h and at 975 °C for 15 min in a vacuum of $2.6 \cdot 10^{-4}$ Pa. All the samples were placed in the furnace at the same time to maintain the same condition. After cooling to room temperature, contact angles were measured by an optical microscope from the geometry of drop images. The measurement error of contact angles is about ±2.5°. The thermal expansion and solidification of the Al droplets during cooling may influence the geometry of the solidified droplet and the measured contact angles, but the effects are within the measurement error.

The surface roughness was measured using a profilometer called Perthometer (Perthen, Mahr), which is a well-known conventional instrument to determine a surface profile and surface roughness. In the measurement, the stylus tip from the Perthometer moves on the sample surface and the surface profile is traced by the displacement of the tip. Three different stylus sizes (2 μm, 5 μm, and 10 μm in radii) were used in the measurements to characterize the rough surfaces. In order to obtain the peak distributions and wavelengths from the profile of the rough surfaces, an ALPHA-STEP 200 (TENCOR Instruments) with a stylus size of 5 μm in radius was used. The average wavelength was measured from the surface profile. All the measurements were repeated for a total of 5 times at both x and y directions on the surface and averaged afterward. Further, a scanning electron microscope (ISI-DS-130) was used to study the rough surface and wetting behavior.

III. EXPERIMENTAL RESULTS

Figure 1 displays a typical SEM image of an Al drop on an Al_2O_3 surface. Figure 2 is the contact edge between Al and Al_2O_3. Obviously the contact angles of Al on the rough surface of Al_2O_3 vary from place to place. The experimental contact angle taken from the geometry of the drop would be the average value of contact angles at the wetting edge.

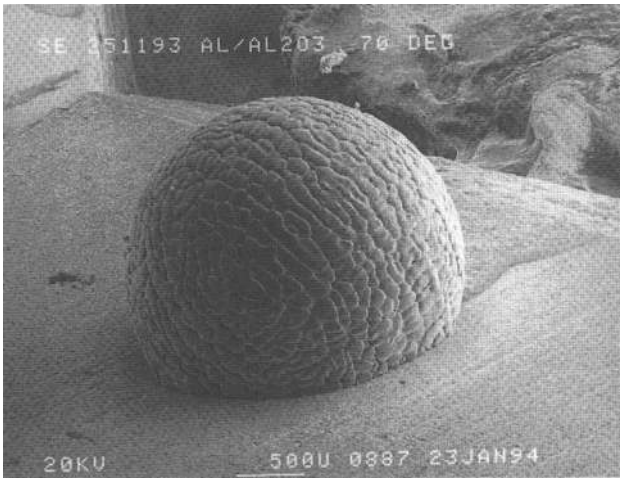

FIG. 1. SEM image of an Al drop on an Al_2O_3 surface.

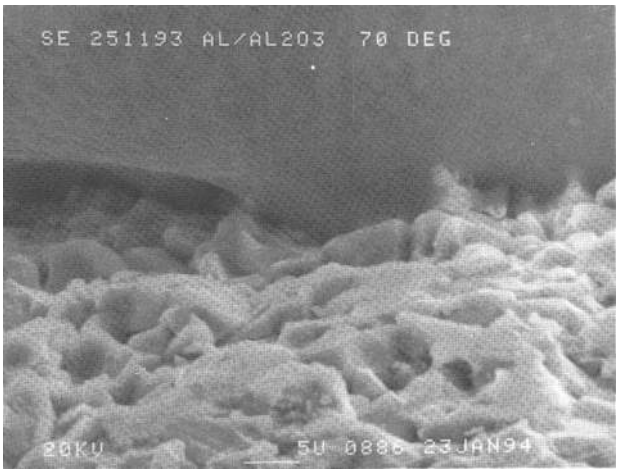

FIG. 2. SEM image of contact edge between an Al drop and an Al_2O_3 surface.

Table I lists the experimental results: contact angles θ_{exp} of liquid Al on solid Al_2O_3 surface at 900 °C and 975 °C, average wavelength λ, and roughness R_a of the Al_2O_3 surface at different stylus sizes r. The measured surface roughness R_a decreases with increasing size r of the stylus. The experimental errors of surface roughness are also listed in Table I. It is noticed that the influence of surface roughness on contact angles is quite significant. With increasing roughness of Al_2O_3 surface, contact angles of liquid Al increase at both 900 °C and 975 °C. Contact angles at 975 °C are much lower than those at 900 °C. It may also be noticed that the contact angles are different even on the same specimen. The differences are larger than the experimental error. The reason for that will be discussed in the following section.

TABLE I. Experimental results of contact angle of liquid Al on Al_2O_3, surface roughness at different stylus sizes (r = 2, 5, and 10 μm), and wavelength.

Samples	Contact angle θ_{exp} (deg)		Roughness R_a (μm)			Wavelength λ (μm)
	At 900 °C	At 975 °C	r = 2 μm	r = 5 μm	r = 10 μm	
A0 received	151.7	96.6, 98.6	0.389 ±0.0396	0.307 ±0.0357	0.0301 ±0.0043	6.424
A1 ground	144.0	89.7, 94.2	0.177 ±0.0269	0.116 ±0.0088	0.0153 ±0.0034	5.256
A2 polished	136.1	84.4, 87.6	0.0466 ±0.0105	0.0259 ±0.0022	0.0058 ±0.0013	2.764
B1 ground	150.6, 168.0	87.3, 101.6	0.238 ±0.019	0.124 ±0.009	0.0182 ±0.0021	4.915
B2 polished	116.2, 124.7	82.1, 86.3	0.0185 ±0.0017	0.0152 ±0.0011	0.00570 ±0.0019	2.285

IV. MODEL

The main purpose of this section is to provide an analytical expression which may correlate conventional roughness parameters with contact angles. The principal assumption of the model is that rough grooves of a surface distribute as a cosine profile with a Gaussian distribution of amplitudes. In this type of groove profile, wavelength and amplitude are the only two parameters to characterize the rough surface. Further, a rough surface can be represented by a combination of two types of grooves: radial grooves an circular grooves, in the middle of which a liquid drop was placed. The effect of radial grooves on contact angles can be treated thermodynamically to attain an equilibrium state, but the circular grooves contribute to the metastable state of wetting. As a result, specific relationships among contact angle, wavelengths, and amplitude of the cosine profile on both radial and circular grooves can be derived. Finally, the relationship between conventional roughness parameters and contact angles is provided by the model.

A. Influence of stylus size on surface roughness value

To imitate a real surface, rough grooves on the surface are assumed to distribute as a cosine profile with a Gaussian distribution of amplitudes A as presented in the following:

$$z = A\cos\left(\frac{2\pi x}{\lambda}\right) \tag{1a}$$

$$P_A = \frac{1}{\sigma_A\sqrt{2\pi}}\exp\left(-\frac{A^2}{2\sigma_A^2}\right) \tag{1b}$$

where x is the position on the surface, z the variation of height, λ the wavelength, A the amplitude, and σ_A the standard deviation A.

The stylus tip that was applied to measure the surface roughness is supposed to have a spherical shape. If a stylus tip with a radius of r moves over a cosine profile of grooves, some parts of the grooves may not be touched or "seen" by the stylus tip because of the finite size effect. The variation of the stylus tip on the cosine profile surface represents the experimentally detected surface profile. According to the definition of the surface roughness,[14] the surface roughness value measured with a finite stylus r can be calculated from the moving trace of the stylus tip center on the surface, as illustrated in Fig. 3:

$$R_r = \int_0^{\infty} 2P_A\left[\frac{2}{\lambda}\int_{x_0}^{\lambda/2}\left|f(x) - \frac{2}{\lambda}\int_{x_0}^{\lambda/2}\right| \times f(x)|dx_1|dx_1\right] dA \tag{2}$$

where

$$f(x) = A\cos\left(\frac{2\pi x}{\lambda}\right) - r + r\cos\left\{\text{arctg}\left[\frac{2\pi A}{\lambda} \times \sin\left(\frac{2\pi x}{\lambda}\right)\right]\right\} \tag{2a}$$

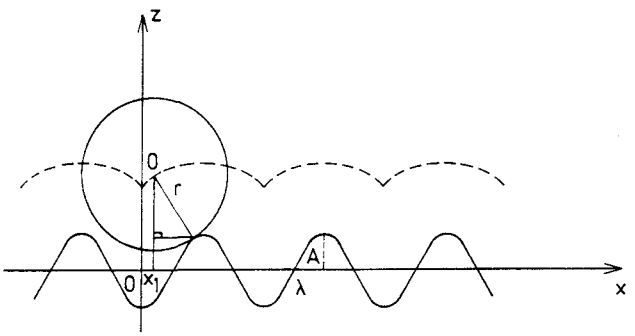

FIG. 3. Variation of a spherical stylus tip moving on a cosine profile surface.

and

$$x_1 = x - r\sin\left\{\text{arctg}\left[\frac{2\pi A}{\lambda}\sin\left(\frac{2\pi x}{\lambda}\right)\right]\right\} \quad (2b)$$

x_1 is the coordinate of the spherical center of the stylus tip, and x_0 is the position of x when $x_1 = 0$. Equation (2) provides the dependence of surface roughness R_r on the stylus size r, standard deviation σ_A of amplitudes A and wavelength λ. After comparison of the experimental roughness R_a with R_r from Eq. (2) at a certain stylus size r, the standard deviation σ_A of amplitudes could be evaluated.

The "real" surface roughness R_{real} of the cosine profile surface measured with an infinite small stylus size can be derived as:

$$R_{\text{real}} = \int_0^{\infty} 2P_A\left[\frac{2}{\lambda}\int_{x_0}^{\lambda/2}\left|A\cos\left(\frac{2\pi x}{\lambda}\right)\right|dx\right]dA$$
$$= \left(\frac{2}{\pi}\right)^{3/2}\sigma_A \approx 0.5\sigma_A \quad (3)$$

which is about half of the standard deviation σ_A and is independent of wavelength λ. R_{real} should be larger than R_r because of the stylus size effect.

B. Wetting on radial grooves

Rough grooves of a surface, which may contribute to the influence of contact angles, can be categorized in two types: radial grooves and circular grooves, in the middle of which a liquid drop is placed.[4] Any practical rough surfaces can be represented by a combination of these two cases. Here we start with a wetting on radial grooves.

Figure 4 illustrates a liquid drop wetted by a rough surface. G is the radius of the liquid drop and H is the height of the drop center from the solid surface.

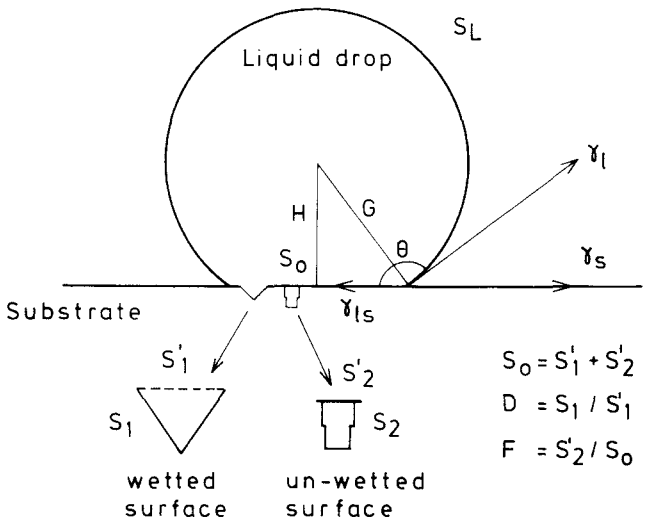

FIG. 4. Definition of the roughness parameters D and F.

The surface area of the liquid drop is given by $S_L = 2\pi G(G + H)$ and the projecting area of the rough interface is $S_0 = \pi(G^2 - H^2)$. If the solid surface is rough, some parts of the interface may be wetted but some may not be. The interface area of wetted parts is S_1 and that of unwetted parts is S_2. The projected areas of S_1 and S_2 on the interface S_0 are S_1' and S_2', respectively, then $S_1' + S_2' = S_0$. Thus two roughness parameters can be defined as $D = S_1/S_1'$ and $F = S_2'/S_0$, where D is the roughness parameter of Wenzel's type[3] and F is that of Cassie and Baxter's type.[6] Obviously $D > 1$ and $F < 1$. With increasing of roughness, both D and F increase. The total energy after wetting may be expressed as follows:

$$E = \gamma_l S_L + \gamma_l S_2' + (\gamma_{ls} - \gamma_s)S_1$$
$$= \pi\gamma_l\{2G(G + H) + (G^2 - H^2)[F - D(1 - F)\cos\theta_{\text{th}}]\} \quad (4)$$

where γ_s, γ_l, and γ_{ls} are the interface energies among solid-vapor, liquid-vapor, and liquid-solid; θ_{th} is the theoretical contact angle defined as $\cos\theta_{\text{th}} = (\gamma_s - \gamma_{ls})/\gamma_l$. The real contact angle θ is given by the geometry of drop image: $\cos\theta = -H/G$. Notice that the liquid drop should be volume preserved, and therefore H and G are functions of θ. If rough grooves of a surface distribute radially, e.g., perpendicular to a wetting triple line, the roughness parameters D and F can be treated as a constant and the equilibrium state of wetting would be achieved. Then the energy minimum condition of $dE/d\theta = 0$ in the complete system can be applied to Eq. (4), resulting in the following formula:

$$\cos\theta_{\text{rad}} = D(1 - F)\cos\theta_{\text{th}} - F \quad (5)$$

where θ_{rad} indicates the contact angle affected by a radial distribution of grooves. If $F = 0$, Eq. (5) reduces to Wenzel's equation[3] and if $D = 1$, it becomes Cassie and Baxter's formula.[6] It should be noticed that Eq. (5) is valid provided the liquid spreads radially on radial grooves of the surfaces.[4] In the case of circular distributed grooves, the equilibrium state in the complete system could not be attained and Eq. (5) would not be met. Actually, the influence of rough grooves on contact angles is effective only at the position of the wetting triple line. This argument of geometry restriction has not been mentioned in Wenzel's treatment.

Now we consider a rough groove having a cosine profile with a Gaussian distribution of amplitudes as described by Eq. (1). In the radial direction of a rough groove, the surface profile does not change. If we place a drop of liquid on this surface, the liquid may wet partly into the cosine profile. The amount of wetted profile can be calculated thermodynamically.

Let us deal with only one wave (one wavelength) of the cosine profile. The energy per unit length of wetting

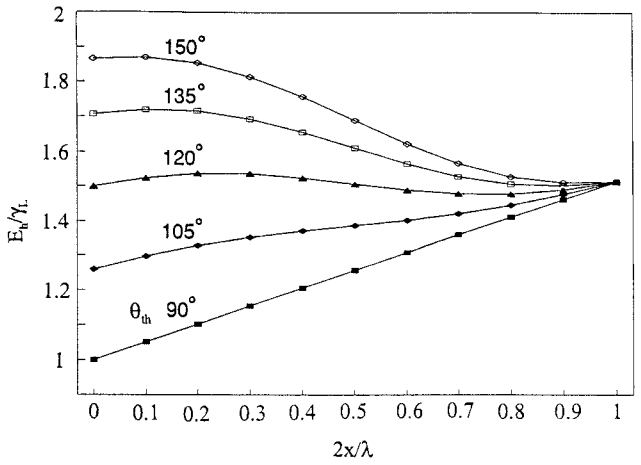

FIG. 5. Energy variation with position x of wetting described by a cosine wave at $A/\lambda = 0.8$.

inside the wave is expressed as:

$$E_h = L_l\gamma_l + L_{ls}\gamma_{ls} - L_{ls}\gamma_s = (L_l - L_{ls}\cos\theta_{th})\gamma_l \tag{6}$$

where L_l is the area of unwetted liquid surface per unit length in the cosine wave, L_{ls} is the curve area of wetted interface per unit length, and θ_{th} is the theoretical contact angle, bearing in mind that the energy E_h is only the local energy inside a rough groove and is different from the energy E in the complete energy as represented by Eq (4). According to the geometry of cosine profile, L_{ls} and L_l can be expressed as follows:

$$L_{ls} = 2\int_x^{\lambda/2}\sqrt{1 + \left[\frac{2\pi A}{\lambda}\sin\left(\frac{2\pi x}{\lambda}\right)\right]^2}\,dx \tag{7a}$$

$$L_l = 2x \tag{7b}$$

Substitution of Eqs. (7) into Eq. (6), the dependence of energy E_h on the position x is obtained. Figure 5 illustrates the energy variation with position x. It can be noticed that there exist both a position of minimum energy and a position of maximum energy at the high contact angle curves (for $\theta > 105°$). The energy peak is a barrier for de-wetting. Assuming that the groove wave is relatively small, then the energy variation inside the wave would not contribute to the total energy of liquid drop during wetting. The minimum condition $dE_h/dx = 0$ can be applied to Eq (6), and the energy minimum position x_t of wetting triple line inside the cosine curve has been derived as:

$$x_t = \frac{\lambda}{2} + \frac{\lambda}{2\pi}\arcsin\left(\frac{\lambda}{2\pi A}\,\mathrm{tg}\theta_{th}\right) \tag{8}$$

where x_t is a function of A and λ as well as θ_{th}. According to the definition of roughness parameters D and F, they can be represented in this case by

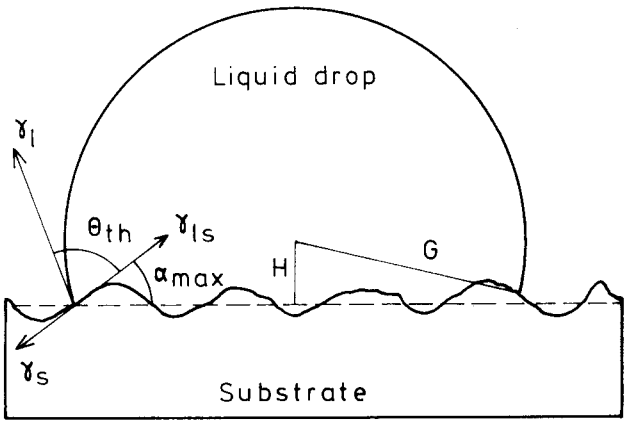

FIG. 6. A cross section of a liquid drop wetted on a rough surface of circularly distributed grooves.

$$D = \int_0^{\infty} 2P_A\left(\frac{L_{ls}}{\lambda - L_l}\right)dA = \int_0^{\infty} 2P_A \times \left\{\frac{2}{\lambda - 2x_t}\int_{x_l}^{\lambda/2}\sqrt{1 + \left[\frac{2\pi A}{\lambda}\sin\left(\frac{2\pi x}{\lambda}\right)\right]^2}\,dx\right\}dA \tag{9a}$$

$$F = \int_0^{\infty} 2P_A\left(\frac{\lambda - L_l}{\lambda}\right)dA = \int_0^{\infty} 2P_A\left(\frac{\lambda - 2x_t}{\lambda}\right)dA \tag{9b}$$

where P_A is represented by Eq. (1b). In Eqs. (9), D and F are not only a function of σ_A and λ but also a function of theoretical contact angle θ_{th}. Therefore D and F should be called surface roughness parameters of wetting. Substitution of the expressions D and F from Eqs. (9) into Eqs. (5), the dependence of contact angle θ_{rad} on σ_A and λ, i.e., on the ratio σ_A/λ, can be evaluated. It should be noticed that this contact angle θ_{rad} is the equilibrium part of the contact angle.

C. Wetting on circular grooves

If wetting on a surface of concentric grooves, in the middle of which a liquid drop is placed as indicated in Fig. 6, an equilibrium state would not be achieved. This type of grooves contributes to the hysteresis behavior of contact angles[7]: an advancing contact angle is larger than a receding contact angle. A maximum advancing contact angle θ_{ad} measured from the image of a liquid drop may be estimated as:

$$\theta_{ad} = \theta_{th} + \alpha_{max} = \theta_{th} + \mathrm{arctg}\left(\left|\frac{dz}{dx}\right|_{max}\right) \tag{10}$$

where α_{max} is the maximum angle of the rough groove and $|dz/dx|_{max}$ is the maximum slope. The minimum

receding contact angle θ_{re} is given by:

$$\theta_{re} = \theta_{th} - \alpha_{max} = \theta_{th} - \text{arctg}\left(\left|\frac{dz}{dx}\right|_{max}\right) \quad (11)$$

The difference between θ_{ad} and θ_{re} is the maximum possible value of the contact angle hysteresis. However, in this wetting experiment, samples were first heated up in order to melt the Al, then the Al liquid drop spread in the advance direction. During cooling the liquid drop was pinned and the contact angle preserved. Therefore the advancing contact angles are more relevant for the experimental contact angles. Thus we take only the advancing contact angle in the later discussion.

In the case of the cosine surface profile with a Gaussian distribution of amplitudes, the maximum advancing contact angle can be derived from Eq. (10):

$$\theta_{ad} = \theta_{th} + \int_0^\infty \left\{2P_A \times \text{arctg}\left[\left|\frac{d\left[A\cos\left(\frac{2\pi x}{\lambda}\right)\right]}{dx}\right|_{max}\right]\right\} \times dA = \theta_{th} + \frac{\sqrt{8\pi}\sigma_A}{\lambda} \quad (12)$$

According to Eq. (12), the roughness parameter σ_A/λ always contributes to an increase of contact angle θ_{ad}, which is different from the effect of roughness on θ_{rad}. As has been pointed out before, a practical rough surface that influences contact angles can be represented by a combination or radial grooves and circular grooves. Therefore the real contact angle of a liquid drop wetted on a rough surface will be between θ_{rad} and θ_{ad}. However, as θ_{ad} is not the equilibrium angle and the distribution of rough grooves may not be homogeneous, then the experimental contact angles would be different even on the same surface. In the case of wetting on a randomly distributed rough surface, an average value θ_{ave} taken from θ_{rad} and θ_{ad} could be more relevant to the average value of experimental contact angles.

D. Calculation and discussion

The correlations among contact angle θ, surface roughness R_r, and wavelength λ have been evaluated by the contribution of Eqs. (2), (5), (9), and (12). It is illustrated in Fig. 7. Figure 8(a) represents the variation of roughness R_r with stylus size r at different values of σ_A and wavelength $\lambda = 4.915$ μm (sample B1) calculated

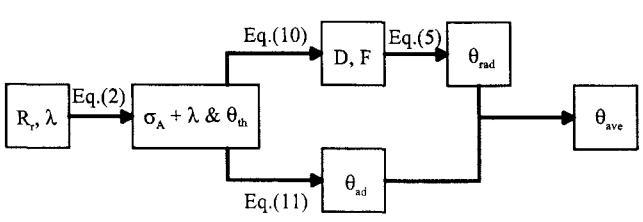

FIG. 7. Correlation between roughness parameters and contact angles by Eqs. (2), (10), (11), and (5) in the model.

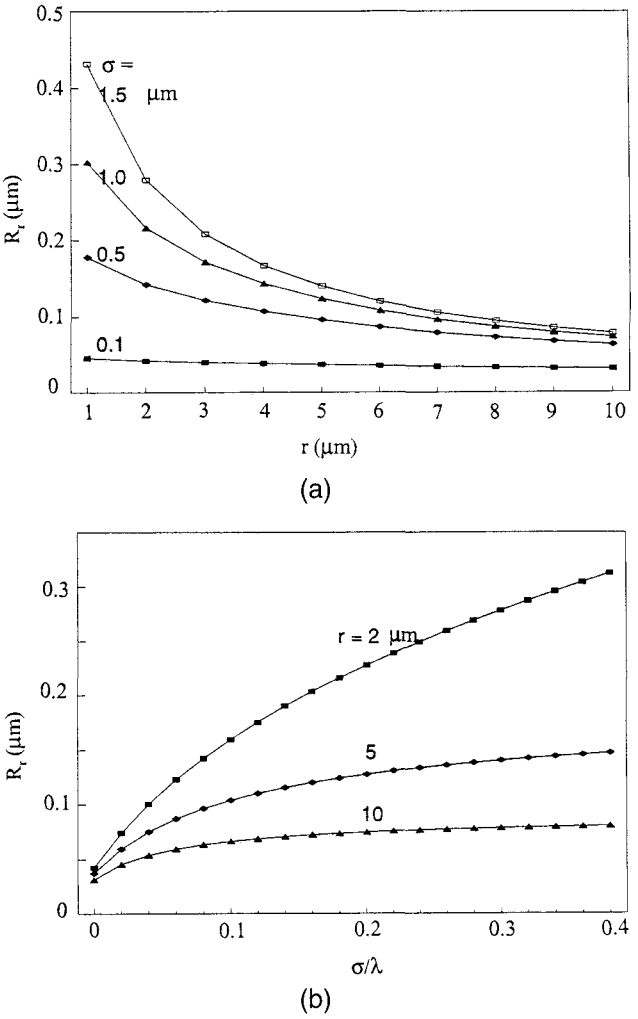

FIG. 8. (a) Dependence of the surface roughness R_r on stylus size r at various σ_A. (b) Dependence on the surface roughness R_r on the ratio σ_A/λ at stylus sizes $r = 2$, 5, and 10 μm. The figure was calculated when $\lambda = 4.915$ μm for sample B1.

from Eq. (2). It can be seen that the roughness R_r varies significantly with the stylus size r. Figure 8(b) represents the dependence of roughness R_r on the ratio of σ_A/λ ($\lambda = 4.915$ μm of sample B) at various stylus sizes $r =$ 2, 5, and 10 μm. Similar figures for other samples with different λ can also be plotted. Taking the experimental roughness from Table I into Fig. 8(b), different values of σ_A/λ ratio at $r = 2$, 5, and 10 μm can be obtained. The σ_A/λ values obtained from Fig. 8(b) are rather similar to each other when $r = 2$ μm and $r = 5$ μm but differ with $r = 10$ μm. This is because if a stylus size r is too large, most features of rough surfaces cannot be characterized. Therefore average values of σ_A/λ at $r =$ 2 μm and $r = 5$ μm have been used in this study which are represented in Table II for various specimens. In the same table "real" roughness R_{real} is also listed as based on the calculation from Eq. (3), which is larger than the experimental roughness R_a.

TABLE II. Calculated results of roughness parameters.

Samples	σ_A/λ	"Real" roughness R_{real} (μm)	At 900 °C			At 975 °C		
			θ_{th} (deg)	D	F	θ_{th} (deg)	D	F
A0 received	0.180	0.589	135	1.109	0.405	85	1.231	1
A1 ground	0.096	0.256		1.070	0.936		1.079	1
A2 polished	0.038	0.054		1.015	1		1.015	1
B1 ground	0.196	0.488	115	1.232	0.947	82	1.264	1
B2 polished	0.020	0.022		1.004	1		1.004	1

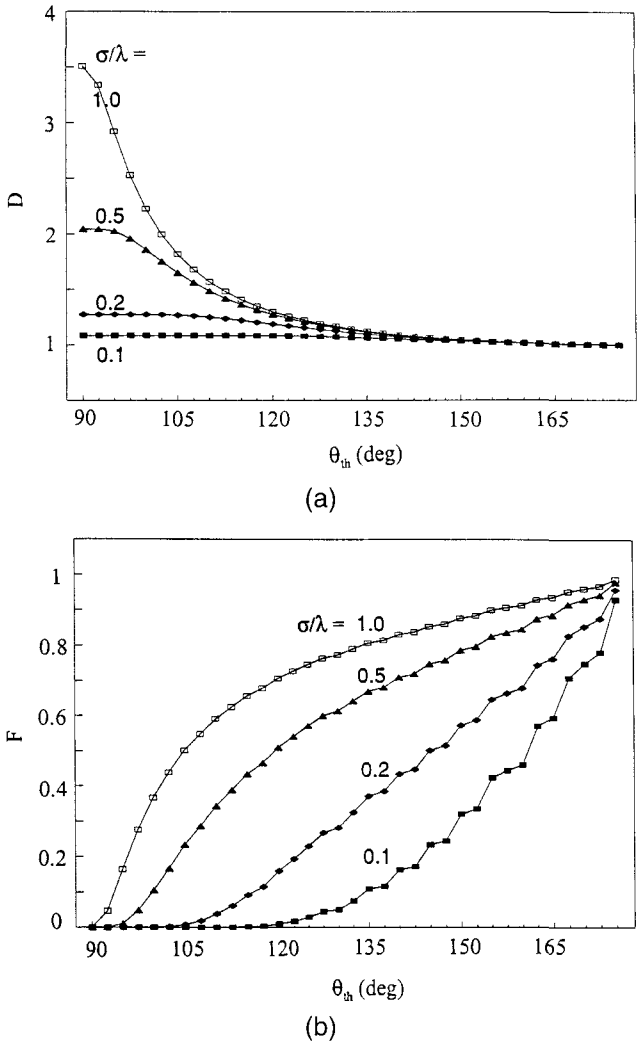

FIG. 9. (a, b) Dependence of the roughness parameters D and F on the theoretical contact angle θ_{th} at various ratios of σ_A/λ.

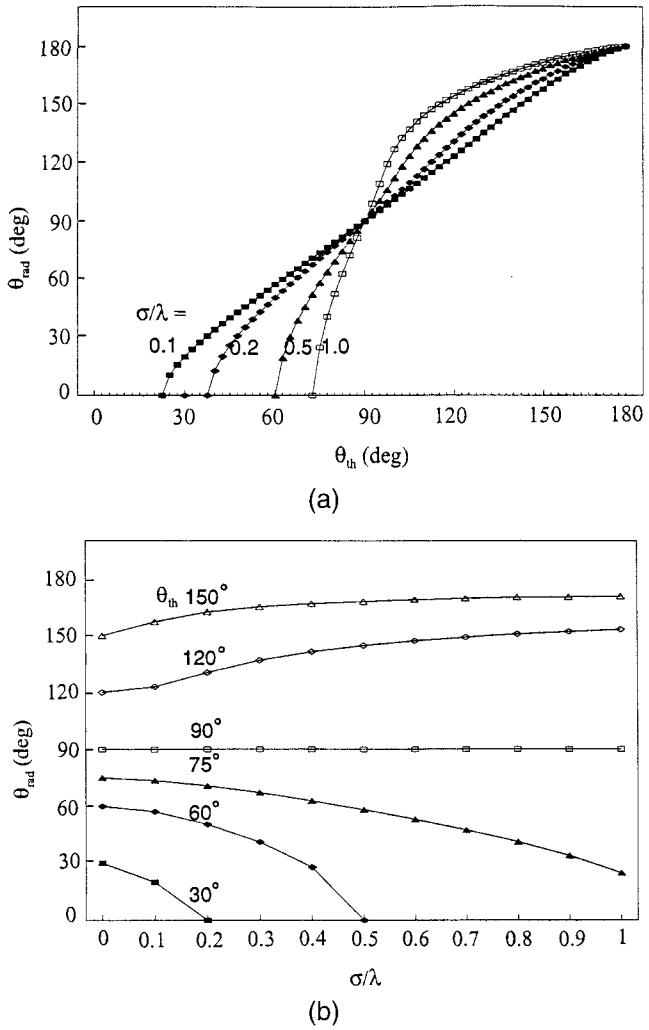

FIG. 10. (a) Dependence of contact angle θ_{rad} on theoretical contact angle θ_{th} at various ratios σ_A/λ. (b) Variation of contact angle θ_{rad} with σ_A/λ at different theoretical contact angles θ_{th}.

Figures 9(a) and 9(b) represent the dependence of roughness parameters D and F on the ratios of σ_A/λ when $\theta_{th} > 90°$, calculated from Eqs. (9). If $\theta_{th} < 90°$, $F = 0$; i.e., the complete interface is wetted and D will not be a function of θ_{th}. Figure 10 illustrates the variation of contact angle θ_{rad} with the theoretical contact angle and σ_A/λ as calculated from Eq. (5). This contact angle θ_{rad} is attributed to the radial grooves. The variation of θ_{rad} with σ_A/λ has a transition at $\theta_{th} = 90°$. When $\theta_{th} > 90°$, θ_{rad} increases with increasing roughness parameter σ_A/λ; when $\theta_{th} < 90°$, θ_{rad} decreases with increasing of σ_A/λ.

Figure 11 illustrates the variation of average contact angle θ_{ave} with the roughness parameter σ_A/λ at various

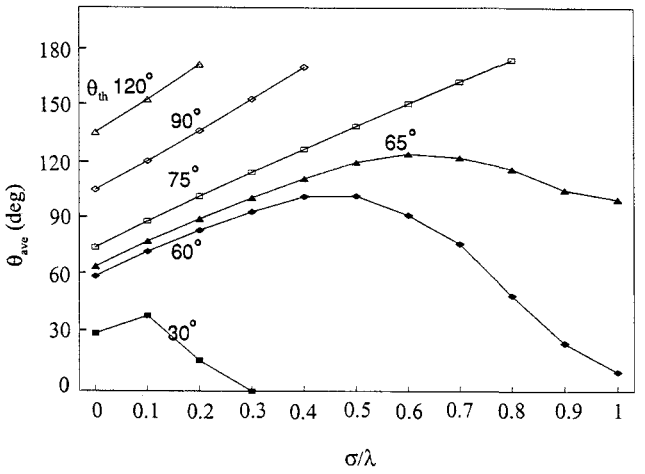

FIG. 11. Variation of contact angle θ_{ave} with σ_A/λ at different theoretical contact angles θ_{th}.

theoretical contact angle θ_{th}, as calculated from the combination of Eq. (5) and Eq. (12). According to this figure, when θ_{th} is larger than about 70°, θ_{ave} increases with increasing σ_A/λ. However, if θ_{th} is smaller than about 70°, the variation of θ_{ave} with σ_A/λ is more complex: when σ_A/λ is small, θ_{ave} increases with increasing of σ_A/λ; when σ_A/λ is large, θ_{ave} decreases with increasing σ_A/λ. Therefore the theoretical contact angle θ_{th} and roughness parameter σ_A/λ are the two key factors to affect contact angles. An interesting example has been reported by Busscher *et al.*[15] In his experiment the transition contact angle is about 73° (instead of 90° as proposed from Wenzel's formula); i.e., with increasing surface roughness, contact angles decrease when θ_{th} is smaller that 73° and increases when θ_{th} is larger than 73°. According to a current model, the deviation of transition contact angle from 90° is induced by the combined effects of radial grooves and circular grooves.

Assuming approximate theoretical contact angles with polished samples, the roughness parameters D and F can be calculated from Eqs. (9) which are listed in Table II for various rough surfaces. The calculated contacted angles θ_{rad}, θ_{ad}, and θ_{ave} are represented in Table III. For the sake of comparison, the experimental contact angles θ_{exp} are also listed in Table III. In the case of wetting at 975 °C, with increasing of surface roughness, θ_{ave} increases but θ_{rad} decreases. Most of the experimental contact angles θ_{exp} lie between θ_{rad} and θ_{ad}. There are a few exceptions which may be caused by the measurement error of surface roughness. θ_{exp} and θ_{ave} are rather close to each other except for sample A0. This is due to the fact that the surface of sample A0 is very rough and the rough grooves distribute inhomogeneously. In conclusion, the model provides a reasonably good estimate for the influence of surface roughness on contact angles.

As contact angles were not measured *in situ* but after cooling and solidification of samples, one might have some doubts about the reliability of the contact angle measurement. The following arguments support the experimental results obtained: (i) According to Fig. 6, which illustrates the energy variation with position when wetting takes place into a rough groove, energy peaks are present. These energy peaks may obscure the de-wetting process. This is consistent with the statement that once a surface is wetted it tends to remain wetted.[16] (ii) In these experiments contact angles of liquid Al on Al_2O_3 measured after cooling and solidification from 900 °C are significantly different from those measured after cooling from 975 °C. It indicates that de-wetting of liquid Al on Al_2O_3 during cooling is slow and might be neglected. Therefore the experimental contact angles of liquid Al on Al_2O_3 measured after cooling and solidification of Al could be a good representation of contact angles at higher temperatures.

The last point for the discussion is the skewness effect. A nonsymmetric distribution of height of a rough surface is called skewness effect.[14] By introducing two different Gaussian distributions of height, a peak distribution with a standard deviation of σ_p and a valley distribution of σ_v, the skewness factor Sk can be expressed as follows according to the skewness definition[14]:

$$Sk = \frac{1}{\sigma^3}\left[\int_{-\infty}^{0} \frac{z^3}{\sigma_v\sqrt{2\pi}} \exp\left(-\frac{z^2}{2\sigma_v^2}\right) dz + \int_{0}^{\infty} \frac{z^3}{\sigma_p\sqrt{2\pi}} \exp\left(-\frac{z^2}{2\sigma_p^2}\right) dz\right]$$

TABLE III. Comparison of contact angles of liquid Al on rough surfaces of Al_2O_3 between experimental measurements and calculated results.

	Contact angle at 900 °C (deg)					Contact angle at 975 °C (deg)				
Samples	θ_{th}	θ_{rad}	θ_{ad}	θ_{ave}	θ_{exp}	θ_{th}	θ_{rad}	θ_{ad}	θ_{ave}	θ_{exp}
A0 received	135	155.9	180.0	168	151.7	85	83.8	136.7	110.3	96.6, 98.6
A1 ground		140.6	162.6	151.6	144.0		84.6	112.6	98.6	89.7, 94.2
A2 polished		135.9	145.9	140.9	136.1		84.9	95.6	90.3	84.4, 87.6
B1 ground	115	123.1	171.3	147.2	150.6, 168.0	82	79.9	138.3	109.1	87.3, 101.6
B2 polished		115.1	120.7	117.9	116.2, 124.7		82.9	87.7	85.3	82.1, 86.3

$$= \sqrt{\frac{2}{\pi}}\left[\left(\frac{\sigma_p}{\sigma}\right)^3 - \left(2 - \frac{\sigma_p}{\sigma}\right)^3\right] \quad (13)$$

where $\sigma = (\sigma_p + \sigma_v)/2$ is the total standard deviation of the height. Upon substitutions of the experimental values of *Sk* into Eq. (13), the ratio of σ_p/σ or σ_v/σ can be calculated. Then two separate cosine profiles have to be introduced in the model mentioned above: one for the peak and another for the valley of a rough surface. However in our experiments, the measured skewness factors *Sk* of Al_2O_3 surfaces are very small ranging from -0.02 to 0.005 and the ratio of σ_p/σ or σ_v/σ is close to one. Therefore the skewness effect to the wetting can be neglected.

V. CONCLUSIONS

Surface roughness has a significant influence on the experimentally determined contact angles of liquid Al on Al_2O_3. In this study of the effects of surface roughness on contact angles, rough grooves can be categorized in two types: radial and circular grooves in the middle of which a liquid drop is placed. Any type of grooves on a practical rough surface is a combination of these two types of grooves. Accordingly a model to predict the effects of surface roughness on contact angles has been proposed. In this model rough grooves are assumed to have a cosine surface profile with a Gaussian distribution of amplitudes. In the comparison with the experimental measurements, the model provides a good estimate for the effects of surface roughness on contact angles of liquid Al on Al_2O_3.

REFERENCES

1. X. B. Zhou and J. Th. M. De Hosson, Acta Metall. Mater. **42**, 1155 (1994).
2. S. W. Ip, M. Kucharski, and J. M. Toguri, J. Mater. Sci. Lett. **12**, 1699 (1993).
3. R. N. Wenzel, Ind. Eng. Chem. **28**, 988 (1936).
4. J. F. Oliver, C. Huh, and S. G. Mason, Colloids and Surfaces **1**, 79 (1980).
5. R. E. Johnson and R. H. Dettre, *Surface and Colloid Science*, edited by E. Matijević (Wiley-Interscience, New York, 1969), Vol. 2, p. 85.
6. A. B. D. Cassie and S. Baxter, Trans. Faraday Soc. **40**, 546 (1994).
7. F. Y. H. Lin, D. Li, and A. W. Neumann, J. Colloid Interface Sci. **159**, 86 (1993).
8. J. Drelich and J. D. Miller, J. Colloid Interface Sci. **164**, 252 (1994).
9. J. De Coninck, Colloids and Surfaces A **89**, 109 (1994).
10. O. N. Tretinnikov and Y. Ikada, Langmuir **10**, 1606 (1994).
11. G. D. Nadkarni and S. Garoff, Europhysics Lett. **20**, 523 (1992).
12. P. Collet, J. De Coninck, and F. Dunlop, Europhysics Lett. **22**, 645 (1993).
13. J. N. Israelachvili, *Intermolecular and Surface Force* (Academic Press, San Diego, CA, 1992), p. 322.
14. T. R. Thomas, *Rough Surfaces* (Longman, London, 1982), pp. 91, 96.
15. H. J. Busscher, A. W. J. van Pelt, P. De Boer, H. P. De Jong, and J. Arends, Colloids and Surfaces **9**, 319 (1984).
16. W. D. Kingery, *Introduction to Ceramics* (John Wiley & Sons, New York, 1960), p. 212.